Tracking Control of Unicycle-Modeled Mobile Robots Using a Saturation Feedback Controller

Ti-Chung Lee, Kai-Tai Song, *Associate Member, IEEE*, Ching-Hung Lee, and Ching-Cheng Teng

Abstract—The tracking control problem with saturation constraint for a class of unicycle-modeled mobile robots is formulated and solved using the backstepping technique and the idea from the LaSalle's invariance principle. A global result is presented in which several constraints on the linear and the angular velocities of the mobile robot from recent literature are dropped. The proposed controller can simultaneously solve both the tracking and regulation problems of a unicycle-modeled mobile robot. With the proposed control laws, the robot can globally follow any path specified by a straight line, a circle or a path approaching the origin using a single controller. As demonstrated, the circular and parallel parking control problem are solved using the proposed controller. Computer simulations are presented which confirm the effectiveness of the proposed tracking control law. Practical experimental results validate the simulations.

Index Terms—Mobile robots, motion control, nonlinear systems, stability, time-varying systems, tracking.

I. INTRODUCTION

CONTROL problems involving mobile robots have recently attracted considerable attention in the control community. Mobile robots with a steering wheel (unicycle) or two independent drive wheels are examples with substantial engineering interest. Most wheeled mobile robots can be classified as nonholonomic mechanical systems. Controlling such systems is, however, deceptively simple. The challenge presented by these problems comes from the fact that a motion of a wheeled mobile robot in a plane possesses three degrees of freedom (DOF); while it has to be controlled using only two control inputs under the nonholonomic constraint. Several researchers indicated, based on Brockett's theorem [9], that such a system is open-loop controllable, but not stabilizable by pure smooth, time-invariant feedback [4], [34]. That is, there does not exist a smooth or continuous feedback law that can stabilize the system.

The methods used in recent years to solve mobile robot control problems can be classified into three categories. The first category is the sensor-based control approach to navigation problems. The emphasis is on interactive motion planning in dynamic environments [43], [46]. Because the working environment for mobile robots is unstructured and may change with time, the robot must use its on-board sensors to cope with the dynamic environment. Most reported designs following this approach rely on intelligent control schemes, such as fuzzy logic control [19] and neural-network learning control [2], [37], [45]. Obstacle motion estimation and environment configuration prediction using sensory information are important for proper motion planning [11], [12]. However, since a mobile robot responds to its surroundings in a reactive or reflexive way; the executed trajectory may not be globally optimized.

In the second category, the navigation problem is decomposed into a path planning phase and a path execution phase. A collision-free path is generated and executed based on a prior map of the environment. The executed path is planned using certain optimization algorithms based on a minimal time, minimal distance or minimal energy performance index. Methods for avoiding both static and moving obstacles have been reported in the literature [15], [16], [24]–[27], [41]. In these methods, a collision-free path is planned according to the environment map space-time relations. The mobile robot must follow the planned path employing a path-following controller.

The third category follows the motion control approach, in which a desired trajectory must be tracked accurately. Among these, tracking controller designs employing a simplified linear model have been reported [4], [13]. Song and Li [44] developed an LQR controller based on a linearized state-space model. In their presentation, the tracking errors can be eliminated and the mobile robot can follow the specified trajectories. In the linear model approach, however, the controller works only when the linear velocity is not zero. Under such circumstances, it would be difficult to control the mobile robot to track the specified trajectory and in the mean time stop with the specified pose. Consequently a more generalized approach is desirable. Nonlinear system theory has been employed to solve this problem [1], [7], [10], [17], [20], [38], [40]. Two main research directions employing nonlinear control design can be distinguished. The first, initiated by Bloch *et al.* [3], [5], used discontinuous feedback, whereas the second research direction used time-varying continuous feedback, which was first investigated by Samson [40]. Pomet [38] then proposed several *smooth* feedback control laws. However, though these solve the regulation problem, they were found to yield slow asymptotic convergence. In order to obtain faster convergence (e.g., exponential convergence), an alternative approach was initially proposed by M'Closkey and Murray [32] and taken up in several subsequent studies (see, e.g., [33]). Our approach falls into this third category.

Research on the tracking problem for mobile robots has been extensive [8], [14], [17], [18], [20]–[22], [29], [30], [36]. Using

T.-C. Lee is with the Department of Electrical Engineering, Ming Hsin Institute of Technology, Hsinchu 300, Taiwan, R.O.C. (e-mail: tc1120@ms19.hinet.net).

K.-T. Song and C.-C. Teng are with the Department of Electrical and Control Engineering, National Chiao Tung University, Hsinchu 300, Taiwan, R.O.C. (e-mail: ktsong@cc.nctu.edu.tw; ccteng@cc.nctu.edu.tw).

C.-H. Lee is with the Department of Electronic Engineering, Lunghwa Institute of Technology, Taoyuan 333, Taiwan, R.O.C. (e-mail: chlee@mail.lhit.edu.tw).

Barbalat's lemma or the backstepping method, control schemes have been proposed for mobile robots to globally follow special paths such as circles and straight lines. Similar results were obtained by Fliess *et al.* [17] using time-reparametrization and the motion-planning properties of differentially flat systems. Despite this apparent advance, there exist several key restrictions on these applications:

1) In some studies on tracking problems [20], [21], [36], [44], only certain special cases (e.g., straight lines or circles) are solved, where the tracked linear velocity v_r or angular velocity w_r must not converge to zero. These restrictions limit the range of applications and, more importantly, make it impossible for a single controller to treat the regulation problem and the tracking problem simultaneously.

2) In other cases [5]–[7], [33], [38], [40], tracking problems with linear and angular velocities approaching zero remain unsolved.

In practical applications, it is preferable to solve the tracking problem and the regulation problem simultaneously using a single controller; otherwise, switching between two different types of controllers will be necessary. In this study, we simultaneously solved the tracking problem and the regulation problem of unicycle-modeled mobile robots without any further assumptions. Moreover, the bounds on the wheel velocities must be attended to avoid the high-gain control signal. The important saturation constraints on control inputs (the linear and angular velocities) were incorporated in our controller design.

Using the backstepping technique, which is often employed in mobile robot stability problems, we will present a global result. With our approach, mobile robots can globally follow any specified path, including straight lines, circles, or trajectories approaching the origin. Furthermore, several important cases, such as parallel parking, can be solved exploiting the proposed method. To the best of the authors' knowledge, in the time-varying continuous feedback literature, this is a here-to-fore unsolved research area. The possibility of extensions to other nonholonomic systems, such as the tracking control of a knife edge, will also be discussed. Simulation results as well as practical experiments will be presented to illustrate the effectiveness of the proposed tracking control law.

The rest of this paper is organized as follows. Section II describes the formulation of the control problem. Our main results, including the control law and the stability analysis are presented in Section III. Section IV illustrates both simulations and experimental results using the proposed tracking controller and a laboratory mobile robot. An extended discussion of the experimental results is presented in Section V. Section VI is the conclusion.

II. PROBLEM FORMULATION

The unicycle-modeled mobile robots considered in this paper are a class of computer-controlled vehicles whose motion can be described or transformed into the following model of constrained movement in a plane:

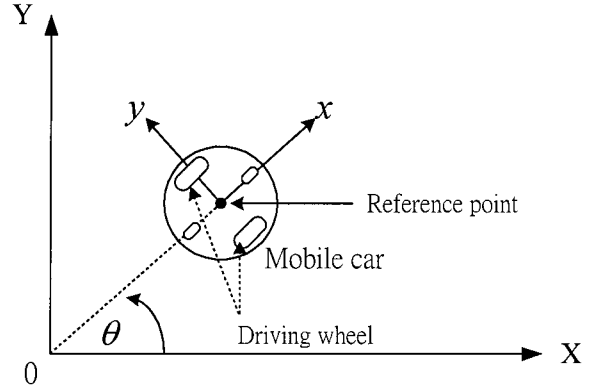$$\begin{aligned} \dot{x} &= v\cos\theta \\ \dot{y} &= v\sin\theta \\ \dot{\theta} &= w \end{aligned} \tag{1}$$

Fig. 1. A nonholonomic mechanical system: unicycle-modeled mobile robot.

where (x, y) are the Cartesian coordinates and θ is the angle between the heading direction and the x-axis. Examples of this model include the widely used front-wheel drive automobiles, automated guided vehicles (AGVs) with a drive and steering wheel (a unicycle) and mobile robots with two independent drive wheels, (see Fig. 1) [35]. Moreover, the knife edge system can also be viewed as an extended unicycle system (1) (see Section V for details). The nonholonomic constraint for the model (1) is

$$\dot{y}\cos\theta - \dot{x}\sin\theta = 0. \tag{2}$$

It specifies the tangent direction along any feasible path for the robot and briefly show that a mobile robot with two independent drive wheels can be described using the unicycle model (1). We assumed that the reference point lies at the midpoint of the two drive wheels. Let v_L and v_R denote the velocities of the left wheel and the right wheel, respectively. The linear velocity v and angular velocity w of the mobile robot can be described as $v = (v_L + v_R)/2$ and $w = (v_R - v_L)/E$, where E represents the distance between two drive wheels. Thus, it is not difficult to see that the mobile robot kinematic equation can be described using the unicycle model (1) (also see the discussion in Section IV). In a plane, the unicycle system possesses three degrees of motion freedom, but must be controlled by only two control inputs under a nonholonomic constraint. When we consider the state vector (x, y, θ), it is straightforward to show that the system (1) is controllable in both position and orientation [35]. Unfortunately, we confront a system where linearization results in a loss of controllability, although the nonlinear system is controllable. In particular, many researchers, based on Brockett's theorem [9], showed that such a system is open-loop controllable, but not stabilizable using the pure smooth time-invariant feedback law [4].

A. Tracking Control Problem with Saturation Constraint

Suppose the reference trajectory (x_r, y_r, θ_r) satisfies

$$\begin{aligned} \dot{x}_r &= v_r\cos\theta_r \\ \dot{y}_r &= v_r\sin\theta_r \\ \dot{\theta}_r &= w_r \end{aligned} \tag{3}$$

where the desired linear velocity $v_r = \sqrt{\dot{x}_r^2 + \dot{y}_r^2}$ satisfies $0 \leq \sup_{t \geq 0} v_r(t) < v_{\max}$, and the desired angular velocity satisfies $\sup_{t \geq 0} |w_r(t)| < w_{\max}$. The desired velocities are bounded and uniformly continuous, with $v_{\max}$ and $w_{\max}$ representing saturation bounds obtained from practical restrictions on control inputs $v(t)$ and $w(t)$, respectively. Note that in the perfect tracking case, i.e., $x \equiv x_r, y \equiv y_r, \theta \equiv \theta_r$, (3) always holds. In this paper, our main purpose is to solve the following tracking problem for (1).

1) Tracking Problem with Saturation Constraint (TPSC): Find saturation control laws for v and w with $|v| < v_{\max}, |w| < w_{\max}$ such that the mobile robot with the kinematic equation (1) follows a reference trajectory $(x_r(t), y_r(t), \theta_r(t))$. That is, $\lim_{t \to \infty} |x(t) - x_r(t)| = 0$, $\lim_{t \to \infty} |y(t) - y_r(t)| = 0$, and $\lim_{t \to \infty} |\theta(t) - \theta_r(t)| = 0$.

Using the robot local frame (i.e., the moving coordinate system x–y in Fig. 1), the error coordinates [23] can be defined as

$$
\begin{bmatrix} x_e \\ y_e \\ \theta_e \end{bmatrix} = \begin{bmatrix} \cos\theta & \sin\theta & 0 \\ -\sin\theta & \cos\theta & 0 \\ 0 & 0 & 1 \end{bmatrix} \begin{bmatrix} x_r - x \\ y_r - y \\ \theta_r - \theta \end{bmatrix}.
$$

Therefore, the tracking error model is obtained

$$
\begin{aligned}
\dot{x}_e &= w y_e - v + v_r \cos\theta_e \\
\dot{y}_e &= -w x_e + v_r \sin\theta_e \\
\dot{\theta}_e &= w_r - w.
\end{aligned} \tag{4}
$$

For convenience, we chose new coordinates and inputs [35] as

$$
\begin{bmatrix} x_0 \\ x_1 \\ x_2 \end{bmatrix} = \begin{bmatrix} \theta_e \\ y_e \\ -x_e \end{bmatrix}, \qquad \begin{bmatrix} u_0 \\ u_1 \end{bmatrix} = \begin{bmatrix} w_r - w \\ v - v_r \cos x_0 \end{bmatrix}.
$$

Equation (4) can be rewritten as

$$
\dot{x}_0 = u_0 \tag{5a}
$$

$$
\dot{x}_1 = (w_r - u_0)x_2 + v_r \sin x_0 \tag{5b}
$$

$$
\dot{x}_2 = -(w_r - u_0)x_1 + u_1. \tag{5c}
$$

With the new coordinates (x_0, x_1, x_2), the tracking problem is now transformed into a stability problem. System (5a)–(5c) is referred as the error model of the TPSC. In the remainder of this paper, the coordinates (x_0, x_1, x_2) will be used in solving the tracking problem. Note that every coordinate transformation used above is invertible, and $(x_0, x_1, x_2) = (0, 0, 0)$ is equivalent to $x = x_r, y = y_r$, and $\theta = \theta_r$. Thus, by invertability of coordinate transformation, if (x_0, x_1, x_2) converges to zero then the TPSC is solved.

Remark 1: The TPSC covers two important cases.

Case 1 (Regulation Case): If $v_r(t) = 0$ and $w_r(t) = 0$, then the TPSC is reduced to the regulation (stability) problem studied in [38].

Case 2 (Tracking Case): If $\lim_{t \to \infty} v_r^2(t) + w_r^2(t) \neq 0$, then the TPSC is reduced to the so-called tracking control problem studied in [20].

It is observed that tracking a straight line or a circular path belongs to Case 2, and the reference trajectory can be described by (3) (see [20] for the straight line case and Section IV for circular paths). However, tracking a path approaching the origin, e.g., the parallel parking problem, has remained unsolved because $v_r^2(t) + w_r^2(t) \neq 0$ for some $t \geq 0$ (violating the condition given in Case 1) and $\lim_{t \to \infty} v_r^2(t) + w_r^2(t) = 0$ (thus not satisfying Case 2).

Remark 2: Because the TPSC covers two different cases, it will not be easy to solve using a single controller. In fact, there are some differences between Cases 1 and 2. For example, consider the following linearized model of (5a)–(5c) at the equilibrium point (0,0,0):

$$
\dot{\overline{x}} = \begin{bmatrix} 0 & 0 & 0 \\ v_r & 0 & w_r \\ 0 & -w_r & 0 \end{bmatrix} \overline{x} + \begin{bmatrix} 1 & 0 \\ 0 & 0 \\ 0 & 1 \end{bmatrix} \begin{bmatrix} \overline{u}_0 \\ \overline{u}_1 \end{bmatrix}.
$$

It can be seen that this linearized model is not stabilizable in Case 1, but stabilizable using the linear feedback controller for the case $v_r^2(t) + w_r^2(t) \geq \varepsilon > 0$ for all $t \geq 0$ (a slightly stronger condition than the condition given in Case 2). On the other hand, the key to study the stability in Case 1 is to use a "persistent excitation" input to u_0, (i.e., $\lim_{t \to \infty} u_0(t) \neq 0$) based on LaSalle's invariance principle [38], while the key to study the stability in Case 2 is to use the "persistent excitation" of $w_r(t)$ and $v_r(t)$ [i.e., $\lim_{t \to \infty} w_r^2(t) + v_r^2(t) \neq 0$] [20]. Note that the persistence of excitation condition is often used to guarantee the stability of an adaptive control system. In the stability issue, the conditions $\lim_{t \to \infty} u_0(t) \neq 0$ and $\lim_{t \to \infty} w_r^2(t) + v_r^2(t) \neq 0$ have the same effect as the persistent excitation discussed in system identification and adaptive control literature. Based on these observations, a possible solution is to find an input u_0 such that $u_0 - w_r$ is "persistent excitation" to solve the TPSC using a single controller in view of (5a)–(5c) and the hint from LaSalle's invariance principle. This idea provided the initial motivation for this study. We will first solve the TPSC for the unicycle model (1) and then apply it to a mobile robot with two-independent drive wheels.

III. GLOBAL TRACKING CONTROL LAWS WITH SATURATION CONSTRAINTS

In this section, a global tracking control law with saturation constraints is derived exploiting the backstepping method and conventional stability theory. The stability of the closed-loop system is guaranteed without any further assumptions relating to v_r and w_r.

First, let us define the saturation function $sat_\delta(x)$ with $\delta > 0$ as

$$
sat_\delta(x) = \begin{cases} x, & \forall |x| \leq \delta \\ \text{sgn}(x)\delta, & \forall |x| > \delta. \end{cases} \tag{6}
$$

Then we define a positive-definite function

$$
V_1(x_1, x_2) = x_1^2 + x_2^2. \tag{7}
$$

Notice that (7) is the square of the distance between the current location of the mobile robot and the desired trajectory. Taking the derivative of V_1 along the trajectory of (5a)–(5c) yields

$$\dot{V}_1 = 2(x_2 u_1 + x_1 v_r \sin x_0). \tag{8}$$

Choosing the saturation control law

$$u_1 = -sat_a(k_0 x_2) \tag{9}$$

where $k_0 > 0$ and $0 < a < v_{\max} - \sup_{t \geq 0} |v_r|$. Note that

$$|v| \leq |u_1| + |v_r \cos x_0| < v_{\max} \tag{10}$$

satisfies the saturation constraint of the linear velocity.

Using the saturation control (9), we have

$$\dot{V}_1 = -2sat_a(k_0 x_2)x_2 + 2x_1 v_r \sin x_0. \tag{11}$$

Next, introduce a new variable

$$\overline{x}_0 = x_0 + \frac{\varepsilon h(t) x_1}{1 + V_1^{1/2}} \tag{12}$$

with $h(t) = 1 + \gamma \cos(\mu t)$, $0 < \gamma < 1$, and $0 < \varepsilon < 1/(1 + \gamma)$. The parameter μ can be chosen as unity if one of the following conditions holds:

$$(C1) \quad \int_0^\infty v_r(t) \, dt = \infty,$$

$$(C2) \quad \lim_{t \to \infty} w_r(t) = 0,$$

$$(C3) \quad \lim_{t \to \infty} \inf |w_r(t)| > 0.$$

In practical applications, one of the conditions (C1)–(C3) must hold, and μ can usually be chosen as one. For example, condition (C1) is satisfied in the straight line and circular path cases; condition (C2) holds for the case of tracking a path approaching the origin. However, for completeness, it is necessary to consider the case in which none of the conditions (C1)–(C3) is satisfied. In this case, μ is chosen as zero. Note that other specifications of the function h in (12) are possible (see Remark 3 after Theorem 1 for details).

We observe that $x_0 \to 0$ as $\overline{x}_0 \to 0$ under the condition that $x_1 \to 0$. Thus, the stability of (x_0, x_1, x_2) can be guaranteed if $(\overline{x}_0, x_1, x_2)$ converge to zero. With (12), system (5a) is transformed into

$$\dot{\overline{x}}_0 = \alpha(x_1, x_2, t)u_0 + \beta(x_0, x_1, x_2, t) \tag{13}$$

where

$$\alpha(x_1, x_2, t) = 1 - \frac{\varepsilon h x_2}{1 + V_1^{1/2}},$$

$$\beta(x_0, x_1, x_2, t) = \varepsilon \left[\frac{\dot{h} x_1 + h w_r x_2 + h v_r \sin x_0}{1 + V_1^{1/2}} \right.$$
$$- \frac{h x_1}{(1 + V_1^{1/2})^2 V_1^{1/2}}$$
$$\left. \cdot (x_1 v_r \sin x_0 - sat_a(k_0 x_2)x_2) \right].$$

It is easy to check that $0 < 1 - \varepsilon(1 + \gamma) \leq \alpha(x_1, x_2, t) < 2$. Choose the control law with saturation constraint u_0 as

$$u_0 = \frac{-\beta(x_0, x_1, x_2, t)}{\alpha(x_1, x_2, t)} - sat_b(k_1 \overline{x}_0) \tag{14}$$

with $k_1 > 0$ and $b > 0$. Then

$$\dot{\overline{x}}_0 = -\alpha(x_1, x_2, t)sat_b(k_1 \overline{x}_0). \tag{15}$$

Note that $\lim_{\varepsilon \to 0^+}(-\beta(\cdot)/\alpha(\cdot)) = 0$. So, it is possible to choose a small $\varepsilon > 0$ and $b > 0$ such that $\sup_{t \geq 0} |u_0| < w_{\max} - \sup_{t \geq 0} |w_r(t)|$. Then $|w(t)| \leq |u_0| + |w_r| < w_{\max}$ satisfies the saturation constraint of the angular velocity. Define $V_2(\overline{x}_0) = \overline{x}_0^2/2$. We then obtain

$$\dot{V}_2 = -\alpha(x_1, x_2, t)sat_b(k_1 \overline{x}_0)\overline{x}_0$$
$$= \begin{cases} -\alpha(x_1, x_2, t)k_1 \overline{x}_0^2, & |k_1 \overline{x}_0| \leq b \\ -\alpha(x_1, x_2, t)b|\overline{x}_0|, & |k_1 \overline{x}_0| > b \end{cases}$$
$$\leq 0 \quad \forall \overline{x}_0 \in \Re. \tag{16}$$

This means that $\lim_{t \to \infty} \overline{x}_0(t) = 0$ (by the Lyapunov stability theorem [42]).

Now, we are in a position to present the main result.

Theorem 1: Consider a unicycle-modeled mobile robot (1). The tracking problem with saturation constraint can be solved using control laws (9) and (14) with $h(t) = 1 + \gamma \cos(\mu t)$, where either $\mu = 0$ or $\mu = 1$ can be specified according to the previous discussion.

Proof: see the Appendix.

Remark 3:

1) The function $h(t)$ can be chosen as $1 + \gamma \lambda(t)$ with $|\lambda(t)| \leq 1$ and $\lim_{t \to \infty} |\chi(t)\dot{\lambda}(t) + w_r(t)| \neq 0$ for all $0 < \delta < |\chi(t)| \leq 1$ [see (A13)]. Obviously, the selection of function $h(t)$ depends on the properties of $w_r(t)$ (see the proof in the Appendix).

2) By coordinate transformation, we have $V_1(t) = (x_r - x)^2 + (y_r - y)^2$. Therefore, the Lyapunov-like function $V_1(t)$ is just the square of the distance between the current position of the mobile robot and the desired trajectory. It is clear that if $V_1(t) \to 0$ then $x_1 \to 0$ and $x_2 \to 0$. Consequently, the mobile robot moves toward the target.

3) If only $v_r(t)$ and $w_r(t)$ are bounded, the same result still holds. A deeper stability analysis is required and the proof is omitted here (see, however, [28]).

4) (Perfect tracking case) If the initial error is zero (the mobile robot is on the tracked trajectory), then it is easy to see that the tracking errors are also equal to zero at any time.

5) If the saturation constraint constants a and b are infinity, then this reduces to a system without saturation constraint. However, in practical systems, there exist constraints on the outputs of the servo motors.

IV. SIMULATIONS AND EXPERIMENTAL RESULTS

Fig. 2 shows the experimental mobile robot developed in our laboratory. It has two independent drive wheels and two casters for balance. The kinematic equation can be described using (1)

Fig. 2. The experimental mobile robot developed in the Intelligent System Control Integration (ISCI) Laboratory of National Chiao Tung University.

Fig. 3. Block diagram of the wheel motor control system.

Fig. 4. The developed tracking controller.

with $v = (v_L + v_R)/2$ and $w = (v_R - v_L)/E$, where E represents the distance between two drive wheels. The proposed controller can be applied to this case with $v_R = v + (wE/2)$ and $v_L = v - (wE/2)$. Therefore

$$\sup_{t \geq 0} \max(v_L, v_R) \leq \sup_{t \geq 0} v + \frac{E}{2} \sup_{t \geq 0} w < v_{\max} + \frac{E}{2} w_{\max}. \tag{17}$$

In this case, $E = 0.54$ m and the velocities of the left wheel and the right wheel satisfy the constraint $\max(v_L, v_R) \leq 0.6$ m/s. Thus, the values of $v_{\max}$ and $w_{\max}$ can be chosen according to the constraint

$$v_{\max} + 0.27 \, w_{\max} \leq 0.6. \tag{18}$$

For v_L and v_R, however, the above inequality is a conservative result. In practical applications, the above condition can be chosen using a simulation procedure. In general, the selection of $v_{\max}$ and $w_{\max}$ would be larger than those determined by condition (18).

The proposed control law was first verified using computer simulations. Practical experimental results on the mobile robot then validated the simulated performance. The robot motion is controlled by adjusting the velocities of the left and right wheels. Two HCTL-1100 motion controller chips from Hewlett–Packard were employed for servo control of the two drive wheels. The integral velocity control mode of the chip was used in the experiments to assure satisfactory dynamic response. Fig. 3 depicts the block diagram of the wheel motor control system. The on-board control computer only needs to send commands to the IC chips, which manage the velocity servo control. The position estimation of the robot is conducted using an odometer, which samples the left and right wheel
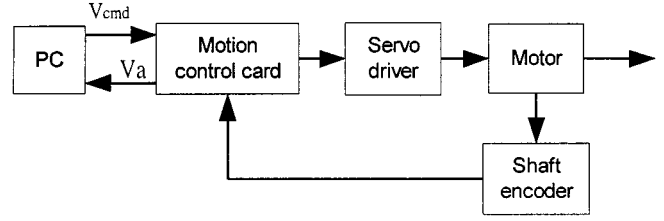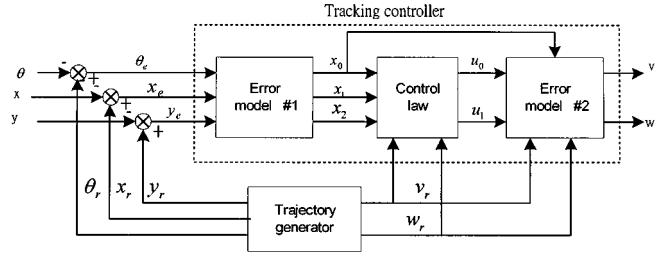
velocities to calculate the current posture of the robot. The formula for this estimator is presented in (19)–(23).

$$v = \frac{v_L + v_R}{2} \tag{19}$$

$$\omega = \frac{v_R - v_L}{E} \tag{20}$$

$$x_{new} = x_{old} + \Delta T \cdot v \cdot \cos(\theta_{old}) \tag{21}$$

$$y_{new} = y_{old} + \Delta T \cdot v \cdot \sin(\theta_{old}) \tag{22}$$

$$\theta_{new} = \theta_{old} + \Delta T \cdot \omega \tag{23}$$

where ΔT is the sampling period. The architecture of the proposed tracking controller is presented in Fig. 4. The models employed in Fig. 4 are described as follows:

- Error Model #1: Equation (5a)–(5c);
- Control law: Equations (9) and (14);
- Error Model #2:

$$\begin{bmatrix} v \\ w \end{bmatrix} = \begin{bmatrix} u_1 + v_r \cos x_0 \\ w_r - u_0 \end{bmatrix}.$$

The desired velocity calculated in the tracking algorithm is transformed into the left and right wheel velocities using

$$v_{rcmd} = v_{out} + \frac{E \cdot w_{out}}{2} \tag{24}$$

$$v_{lcmd} = v_{out} - \frac{E \cdot w_{out}}{2}. \tag{25}$$

Fig. 5 depicts the implemented tracking control system, which was constructed using the proposed algorithm.

Two trajectories were selected to verify the performance of the proposed control law. In the circular-path trajectory, the tracking performance can be examined. The regulation performance can be further checked with the parallel-parking trajectory. The parameters $(k_0, k_1, \gamma, \varepsilon)$ are determined by considering the desired tracking performance. In general, large values for k_0 and ε will result in a fast convergence rate

$$signal: \quad \bar{I}=\begin{bmatrix} x \\ y \\ \theta \end{bmatrix}, \quad \bar{I}_e=\begin{bmatrix} x_e \\ y_e \\ \theta_e \end{bmatrix}, \quad \bar{I}_{r1}=\begin{bmatrix} x_r \\ y_r \\ \theta_r \end{bmatrix}, \quad \bar{I}_{r2}=\begin{bmatrix} v_r \\ \omega_r \end{bmatrix}, \quad \bar{v}=\begin{bmatrix} v \\ \omega \end{bmatrix}, \quad \bar{v}_{out}=\begin{bmatrix} v_{out} \\ \omega_{out} \end{bmatrix}, \quad \bar{v}_{cmd}=\begin{bmatrix} v\_rcmd \\ v\_lcmd \end{bmatrix}$$
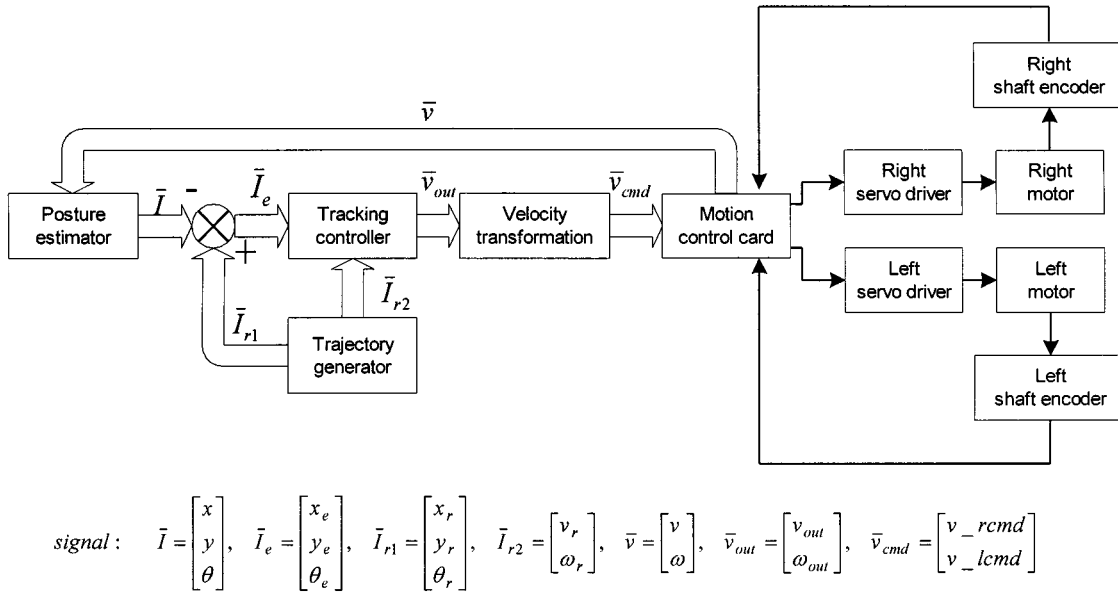
Fig. 5.   The implemented tracking control system.

[see the proof of Theorem 1 in the Appendix for the case of $\int_0^\infty v_r(t)\,dt = \infty$]. In addition, the convergence rate is slightly affected by the parameters k_1 and γ. Experience gained from computer simulations suggested a choice of γ near 0.5. In the following, tracking as well as docking performance is presented for circular and parallel parking trajectories, respectively. The simulation and experimental results are presented in the same figure for comparison. The models that generate the trajectories are illustrated below

■ Circular path:

$$x_r = x_c + R \cdot \sin(e \cdot t) \tag{26a}$$

$$y_r = y_c - R \cdot \cos(e \cdot t) \tag{26b}$$

$$\theta_r = e \cdot t \tag{26c}$$

$$v_r = e \cdot R \tag{26d}$$

$$w_r = e \tag{26e}$$

where (x_c, y_c) represents the coordinate of the center and R is the radius of the circle. In the simulation and experiment, the constants e and R are chosen as $e = 0.5$ and $R = 0.8$ m and are shown in (27a)–(27e) at the bottom of the next page. Fig. 6 illustrates the parking place and the designed trajectory. An "8"-shaped trajectory was employed, where 2a and b represent the long and short axis, respectively. In the simulation and experiment, $a = 0.4$ m, $b = 0.4$ m, and $c = 0.02$. It is easy to check that the above two trajectories 26(a)–26(c) and 27(a)–27(c) satisfy the system (3), with the v_r and w_r given by 26(d)–26(e) and 27(d)–27(e) respectively. Thus, they are perfect tracking cases.

The parameters used in the experiments are presented in Table I. The outputs of the controller were limited as shown in the table, in accordance with the hardware structure of the experimental mobile robot.

For these two cases $h(t)$ can be chosen as $h(t) = 1 + \gamma \cos t$, because the first path satisfies condition (C1) and the second
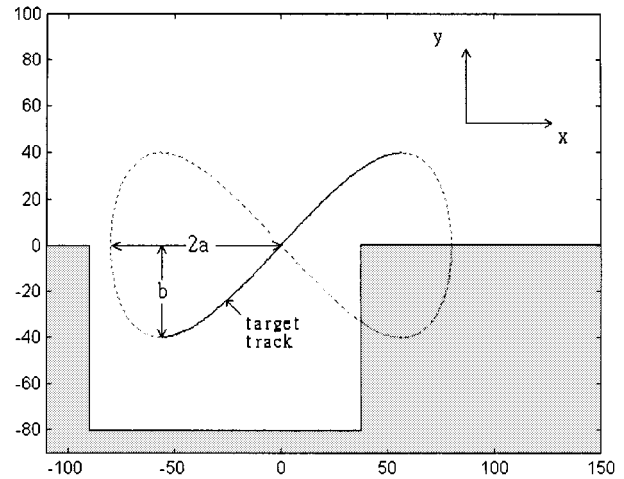

Fig. 6.   The parallel parking place and the designed trajectory.

TABLE I
THE PARAMETERS USED IN THE SIMULATION AND EXPERIMENTS

k_0	k_1	γ	ε	v_{max}	w_{max}
1	1	0.5	0.5	0.33 (m/sec)	1 (rad/sec)

path satisfies condition (C2). Simulation results as well as experimental results with saturation constraints for the circular path and parallel parking are presented in Figs. 7 and 8, respectively. In these figures, the dotted lines represent computer simulation results and the solid lines represent the corresponding experimental results. In Figs. 7(a) and 8(a), we see that the robot trajectories converge to the desired trajectories. These results demonstrate the capacity of the proposed controllers to produce a nice convergence. The marks in Fig. 7(a) indicate respectively the vehicle and target positions when the target is at the starting point of each lap. In this figure, Si and Ei, $i = 1 \sim 5$, are the corresponding positions when the target comes to the starting

point at the lap #i for the simulation and experiment, respectively. We observe that the vehicle tracked the target in the fifth lap. Figs. 7(b) and 8(b) reveal that three tracking errors all converge to zero as expected. Figs. 7(c)–(d) and 8(c)–(d) show the recorded controller outputs, namely, the linear velocity and the angular velocity of the vehicle. These outputs are within the limits set in the controller. As shown in Fig. 8, the instant is indicated when the vehicle reached the docking point ($t = \pi/2c$, with $c = 0.02$). It is observed in Fig. 8(b) and (d) that the experimental system shows a slight oscillatory behavior at the docking point. This is caused by the 8-bit resolution of the velocity command used in the experimental system. Note that the oscillation peak of about 0.05 rad/s is practically at the limit of the command resolution. This quantization error in the practical digital control system also resulted in a small orientation error of about 0.05 rad as shown in Fig. 8(b).

It can be seen from Fig. 7 that the experimental results are better than the simulation results. This is due to the mechanical damping of the practical system and in part by the cyclical characteristic of the circular path. As shown in Fig. 7(a), the experimental trajectory did not match the simulation result in the beginning. In fact the mobile robot approached the desired circular path in the inner side with a slower response than that in the simulation, caused by the damping effect. At a later stage, as the target repeated its trajectory in a circle, the tracking controller worked to eliminate the tracking errors and the robot tracked the target. This particular situation resulted in smaller tracking errors in the experiment than in the simulation. From Figs. 7 and 8, we observed that the tracking errors all approach zero and the mobile robot follows the desired path. These results confirm the

conclusion in Remark 3 (perfect tracking case). To the authors' best knowledge, the problems associated with the parking case, with v_r and w_r approaching zero, was previously unsolved in the literature using the nonlinear theory approach. This research effort has proven that the problem can be solved exploiting the proposed controllers (9) and (14). From the proof of Theorem 1, it is observed that the tracking errors converge to zero exponentially if the target keeps moving. However, if the target stops at some point (regulation case) then the tracking errors decay slowly. In this instance, the TPSC is reduced to a regulation problem. Therefore, a discontinuous or nonsmooth controller is required for fast convergence. For details see [32], [33]. However, the proposed controllers in this paper are smooth controllers. It is strongly suggested that proper controller parameters should be chosen to produce fast convergence so that the desired path is followed before the target stops.

In this study, for the purpose of comparison, the tracking control problem without any constraint on velocities has also been solved employing a single controller. Fig. 9 presents the experimental results of tracking a circular path. It is observed from Fig. 9 that a large control effort and oscillatory transient occurred when the mobile robot was controlled by a nonsaturation controller. On the other hand, satisfactory tracking results were obtained using the proposed saturation controller.

This paper only considers the kinematic model of mobile robots. The dynamic model is not included in the main results of this presentation in order to simplify our discussion. It is known that this simplification is acceptable when the system velocities are low, as is in most mobile robot applications. Extending the results for the kinematic model (1) to the dynamic model is

■ Parallel Parking:

$$x_r(t) = \begin{cases} 2a\cos\left(c\left(t + \frac{\pi}{4c}\right)\right), & 0 \le t \le \frac{\pi}{2c} \\ -a\sqrt{2}, & \frac{\pi}{2c} \le t \end{cases} \tag{27a}$$

$$y_r(t) = \begin{cases} b\sin\left(2c\left(t + \frac{\pi}{4c}\right)\right), & 0 \le t \le \frac{\pi}{2c} \\ -b, & \frac{\pi}{2c} \le t \end{cases} \tag{27b}$$

$$\theta_r(t) = \begin{cases} \pi - \tan^{-1}\left(\frac{b\cos(2c(t + \pi/4c))}{a\sin(c(t + \pi/4c))}\right), & 0 \le t \le \frac{\pi}{2c} \\ \pi, & \frac{\pi}{2c} \le t \end{cases} \tag{27c}$$

$$v_r(t) = \begin{cases} 2c\sqrt{a^2\sin^2\left(c\left(t + \frac{\pi}{4c}\right)\right) + b^2\cos^2\left(2c\left(t + \frac{\pi}{4c}\right)\right)}, & 0 \le t \le \frac{\pi}{2c} \\ 0, & \frac{\pi}{2c} \le t \end{cases} \tag{27d}$$

$$w_r(t) = \begin{cases} \dfrac{abc\left(\cos\left(c\left(t + \frac{\pi}{4c}\right)\right)\cos\left(2c\left(t + \frac{\pi}{4c}\right)\right) + 2\sin\left(c\left(t + \frac{\pi}{4c}\right)\right)\sin\left(2c\left(t + \frac{\pi}{4c}\right)\right)\right)}{\left(a\sin\left(c\left(t + \frac{\pi}{4c}\right)\right)\right)^2 + \left(b\cos\left(2c\left(t + \frac{\pi}{4c}\right)\right)\right)^2}, & 0 \le t \le \frac{\pi}{2c} \\ 0, & \frac{\pi}{2c} \le t. \end{cases} \tag{27e}$$
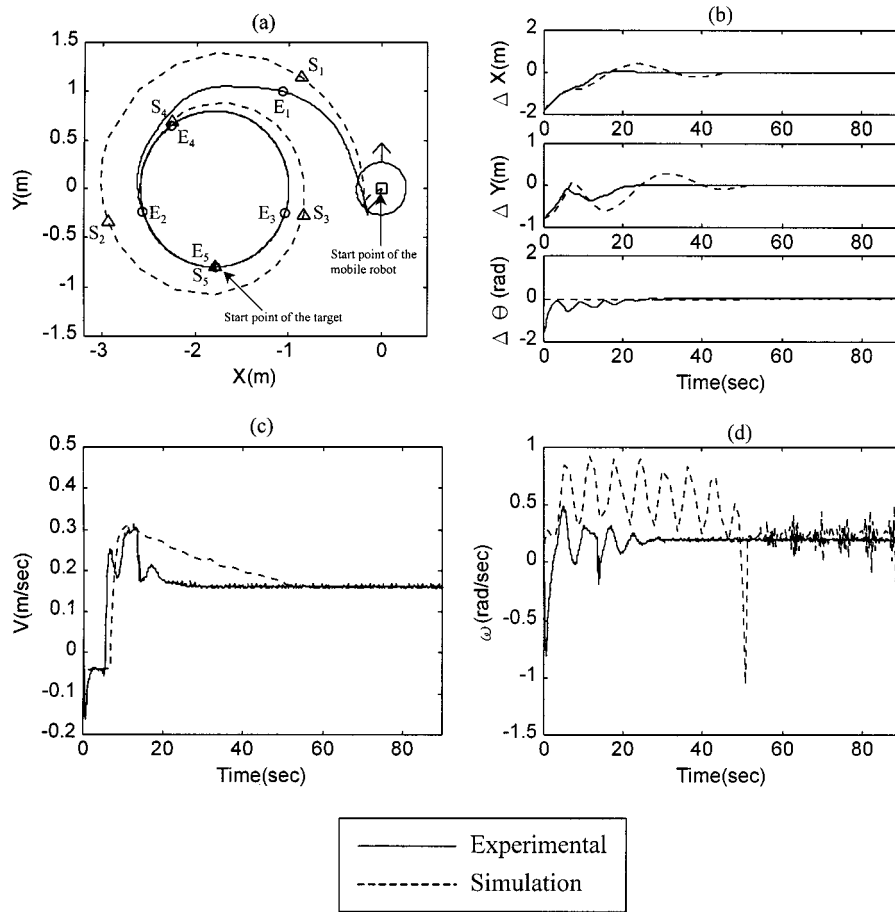
Fig. 7. Experimental and simulation results of tracking a circular trajectory. (a) Position variations. (b) Tracking errors. (c) Linear velocity of the center point. (d) Angular velocity.

possible using the backstepping method (see the discussion in Section V). It can be seen from the experimental results shown in Fig. 7(c) and (d) that robot dynamics affect system performance. Note that the mechanical damping helps to produce a stable, smooth tracking performance. Another factor affecting the experimental performance is the lower-level servo loops. The servo loops have dynamics and the steady-state output of the motors cannot be achieved instantaneously. Normally, this can be managed by proper selection of the sampling time for the tracking controller. In this case, the dynamics and servo stability are assured by implementing the integral velocity control mode of HCTL-1100 motion controller chip.

V. EXTENSION OF THE PROPOSED METHOD

The controller design presented in this paper can be generalized to other control systems of engineering interest, e.g., the control of a knife edge. We now briefly describe the application to a knife edge moving in point contact on a plane surface [4]–[7]. With all numerical constants set to unity, the equations of motion are given by

$$\ddot{x} = \lambda \sin \phi + u_1 \cos \phi$$
$$\ddot{y} = -\lambda \cos \phi + u_1 \sin \phi$$
$$\dot{\phi} = u_2 \tag{28}$$

where x and y denote the coordinates of the point of contact of the knife edge in the plane and ϕ is the heading angle of the knife edge, measured from the x-axis; u_1 denotes the control force in the direction defined by the heading angle, u_2 represents the control torque about the vertical axis through the point of contact and λ represents the constraint force. The constraint force components arising from the scalar nonholonomic constraint are described as in (2)

$$\dot{x} \sin \phi - \dot{y} \cos \phi = 0.$$

After coordinate transformation, the differential equations can be reduced to an ordinary fifth-order differential equation [4]. Employing the backstepping technique, this control problem can also be solved. We sketch the approach briefly. Let $v = \dot{x} \cos \phi + \dot{y} \sin \phi$ and $w = \dot{\phi} = u_2$. Equation (28) can be transformed into

$$\dot{x} = v \cos \phi \tag{29a}$$
$$\dot{y} = v \sin \phi \tag{29b}$$
$$\dot{\phi} = w \tag{29c}$$
$$\dot{v} = u_1. \tag{29d}$$

This is a dynamic system that includes an acceleration term. Let $v^* = \psi(x, y, \phi, t)$ and $w^* = \varphi(x, y, \phi, t)$ be two con-
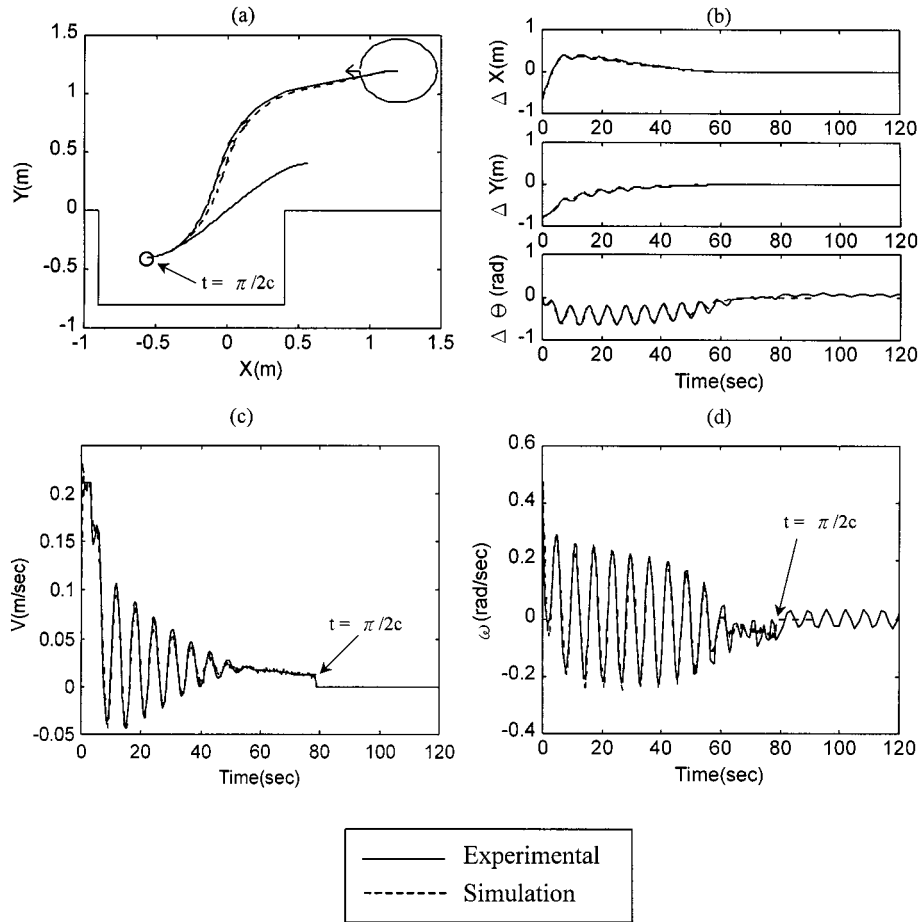
Fig. 8.   Experimental and simulation results of parallel parking. (a) Position variations. (b) Tracking errors. (c) Linear velocity of the center point. (d) Angular velocity.

trollers derived from Theorem 1, where we replace the saturation function $sat_\delta(x)$ by $\delta \tanh x$. Then, $\psi(x, y, \phi, t)$ is differentiable and the same result as in Theorem 1 holds. Therefore, the knife edge control solution can be designed as $u_2 = w^*$ and $u_1 = -k_1(v - v^*) + \dot{v}^*$. A similar approach can be applied to study the mobile robot dynamic model with two independent drive wheels using the backstepping method. The details are omitted due to limited space.

On the other hand, it is also interesting to investigate how to extend the results in this paper to more general driftless systems, e.g., the nonholonomic chained-form systems [35]. However, it seems the approach adopted in this study is not feasible for application to a general chained-form system with order higher than three. The reasons are stated in the following. First, let us briefly discuss the approach adopted in this paper. Note that the function $\sin x_0$ appearing in (5b) can be approximated by x_0 when x_0 is small. Thus, a stabilizing virtual controller x_0^* can be chosen as $x_0^* = (-\varepsilon h x_1 / (1 + V_1^2))$ such that $\dot{V}_1 < 0$ in case of $V_1 \neq 0$ and $v_r > 0$ by equation (11). Then, the backstepping method can be used to guarantee the stability of the whole closed-loop system by choosing a suitable controller u_0 such that the virtual error state $x_0 - x_0^* = \overline{x}_0$ [defined by (12)] converges to zero, see equation (15). Indeed, a similar argument can be performed for the chained-form systems with order three. This is not the case for chained-form systems having order

higher than three. In fact, it is possible to derive a similar error model like (5a)–(5c) for a general chained-form system with order $n > 3$, however, the nonlinear function x_0^2 will also appear in the error model. The application of the backstepping method in this case will not be straightforward. Thus, it is a challenge to achieve a similar result for chained-form systems or more general driftless systems.

VI. CONCLUSION

A single controller was developed to simultaneously solve the tracking and regulation problems of a mobile robot. Experimental results confirm that the proposed saturation feedback controller gives tracking responses within the physical velocity limitations of the employed mobile robot. It was observed that the executed trajectories were smooth even though the specified trajectory contained nondifferentiable discontinuities. Several directions are interesting for future investigation. The combination of sensor-based navigation algorithms with our proposed tracking controller would give a smooth and precise trajectory in dynamic environments. A recent study on this new area was reported by Ma *et al.* [31] combining a vision system with the navigation of a nonholonomic mobile robot. Extending the present result to general chained-form systems remains a challenge for controller design.
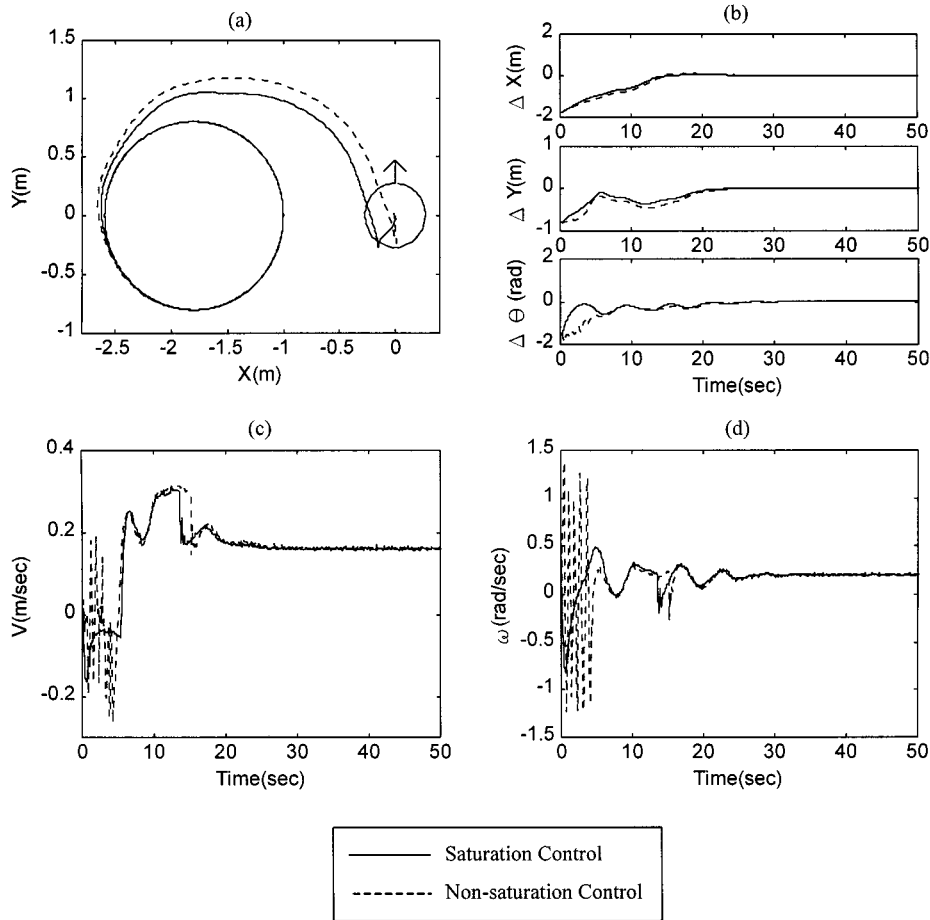
Fig. 9.   Experimental result: comparison of saturation controller and nonsaturation control for tracking a circular trajectory. (a) Position variations. (b) Tracking errors. (c) Linear velocity of the center point. (d) Angular velocity.

APPENDIX
PROOF OF THEOREM 1

A. Several Useful Lemmas

Several technical lemmas, which will be used in the proof of the main results, are described below.

Lemma 1: (Barbalat's lemma, [42]) If f: $\Re^+ \rightarrow \Re$ is uniformly continuous and $\int_0^\infty |f(t)|\,dt$ is finite, then $\lim_{t \to \infty} f(t) = 0$.

Lemma 2: (Reference [20]) Consider the following system:

$$\dot{a}(t) = -ka(t) + b(t)$$

where $k > 0$ and $b(t)$ is bounded and uniformly continuous. If there is a bounded solution $a(t)$ solving the above ordinary differential equation, we have $\lim_{t \to \infty} b(t) = 0$.

Lemma 3: (Reference [39]) Let $f(\cdot, \cdot)$: $\Re^n \times \Re^m \rightarrow \Re$ be a continuous function. If $a(t)$: $\Re^+ \rightarrow \Re^n$ and $b(t)$: $\Re^+ \rightarrow \Re^m$ are two bounded functions with $a(t) \rightarrow 0$, we have $f(a(t), b(t)) \rightarrow f(0, b(t))$.

For the proofs of Lemmas 1–3, readers may refer to [20], [39], [42]. In the following, two more lemmas relating useful differential inequalities are presented. They will be used in the proof of Theorem 1.

Lemma 4: Suppose $a(t) \geq 0$, $b(t) \geq 0$, and $c(t) \geq 0$ for all $t \geq 0$. Consider the following inequality:

$$\dot{a}(t) \leq -b(t) + c(t)a^{1/2}(t) \qquad \forall\, t \geq t_0 \geq 0. \qquad \text{(A1)}$$

If $\int_{t_0}^\infty c(t)\,dt < \infty$, then the following inequalities hold:
1)

$$a^{1/2}(t) \leq a^{1/2}(t_0) + \tfrac{1}{2}\int_{t_0}^t c(t)\,dt \qquad \forall\, t \geq t_0 \geq 0;$$

2)

$$\int_{t_0}^\infty b(t)\,dt < \infty.$$

Proof of Lemma 4:

1) Let ε be any positive constant. First claim that

$$a^{1/2}(t) < a^{1/2}(t_0) + \tfrac{1}{2}\int_{t_0}^t c(t)\,dt + \varepsilon$$

for all $t \geq t_0$. If the claim is false, let $\overline{t_0}$ be

$$\inf_{t \geq t_0}\left\{ t \,\middle|\, a^{1/2}(t) \geq a^{1/2}(t_0) + \tfrac{1}{2}\int_{t_0}^t c(t)\,dt + \varepsilon \right\}.$$

Then, it is clear that

$$a^{1/2}(\overline{t_0}) = a^{1/2}(t_0) + \tfrac{1}{2} \int_{t_0}^{\overline{t_0}} c(t)\, dt + \varepsilon.$$

This results in $\overline{t_0} > t_0$ and $a(\overline{t_0}) > 0$. Moreover, there is a positive constant δ with $\delta < \overline{t_0} - t_0$ such that $a(t) > 0$ and

$$a^{1/2}(t) < a^{1/2}(t_0) + \tfrac{1}{2} \int_{t_0}^{t} c(t)\, dt + \varepsilon$$

for all $\overline{t_0} - \delta t < \overline{t_0}$.

From (A1)

$$\dot{a}(t) \le -b(t) + c(t) a^{1/2}(t) \le c(t) a^{1/2}(t) \qquad \forall\, t \ge t < \overline{t_0}.$$

This implies

$$\int_{\overline{t_0} - \delta}^{t} \frac{\dot{a}(\tau)}{a^{1/2}(\tau)}\, d\tau \le \int_{\overline{t_0} - \delta}^{t} c(\tau)\, d\tau \qquad \forall \overline{t_0} - \delta \le t \le \overline{t_0}.$$

Thus,

$$a^{1/2}(\overline{t_0}) \le a^{1/2}(\overline{t_0} - \delta) + \tfrac{1}{2} \int_{\overline{t_0} - \delta}^{\overline{t_0}} c(t)\, dt$$

$$< a^{1/2}(t_0) + \tfrac{1}{2} \int_{t_0}^{\overline{t_0}} c(t)\, dt + \varepsilon$$

and we reach a contradiction. Therefore, the claim is true for all $\varepsilon > 0$. This implies that 1) holds.

2) From 1) and $\int_{t_0}^{\infty} c(t)\, dt < \infty$, $\mathrm{A} = \max_{t \ge t_0} a(t) < \infty$. Therefore, (A1) can be rewritten as

$$\int_{t_0}^{t} \dot{a}(\tau)\, d\tau \le - \int_{t_0}^{t} b(\tau)\, d\tau + \mathrm{A}^{1/2} \int_{t_0}^{t} c(\tau)\, d\tau. \qquad (A2)$$

By (A2) and $\int_{t_0}^{\infty} c(t)\, dt < \infty$, we obtain

$$\lim_{t \to \infty} a(t) + \int_{t_0}^{\infty} b(\tau)\, d\tau \le a(t_0) + \mathrm{A}^{1/2} \int_{t_0}^{\infty} c(\tau)\, d\tau < \infty$$

and consequently

$$\int_{t_0}^{\infty} b(\tau)\, d\tau < \infty.$$

This completes the proof. ∎

Lemma 5: Suppose $a(t) \ge 0$, $b(t) \ge 0$, and $c(t) \ge 0$ for all $t \ge t_0 \ge 0$. Assume that $b(t)$ is bounded. Consider the following inequality:

$$\dot{a}(t) \le -b(t) a(t) + c(t) \qquad \forall\, t \ge t_0 \ge 0. \qquad (A3)$$

If $\int_{t_0}^{\infty} c(t)\, dt < \infty$ and $\int_{t_0}^{\infty} b(t)\, dt = \infty$, $\lim_{t \to \infty} a(t) = 0$.

Proof of Lemma 5: Let us consider the inequality $\dot{a}(t) \le -b(t) a(t) + c(t)$. Multiplying the term in (A3) by the integral factor $\exp(\int_{s}^{t} b(\tau)\, d\tau)$ with $t \ge s \ge t_0 \ge 0$, we have

$$\exp\left(\int_{s}^{t} b(\tau)\, d\tau \right) \dot{a}(t) + \exp\left(\int_{s}^{t} b(\tau)\, d\tau \right) b(t) a(t)$$

$$\le \exp\left(\int_{s}^{t} b(\tau)\, d\tau \right) c(t)$$

and

$$\frac{d\left\{ \exp\left(\int_{s}^{t} b(\tau)\, d\tau \right) a(t) \right\}}{dt} \le \exp\left(\int_{s}^{t} b(\tau)\, d\tau \right) c(t).$$

So, we have

$$\exp\left(\int_{s}^{t} b(\tau)\, d\tau \right) a(t) - a(s)$$

$$\le \int_{s}^{t} \exp\left(\int_{s}^{\tau} b(\zeta)\, d\zeta \right) c(\tau)\, d\tau. \qquad (A4)$$

Thus

$$a(t) \le \exp\left(-\int_{s}^{t} b(\tau)\, d\tau \right) a(s) + \exp\left(-\int_{s}^{t} b(\tau)\, d\tau \right)$$

$$\cdot \int_{s}^{t} \exp\left(\int_{s}^{\tau} b(\zeta)\, d\zeta \right) c(\tau)\, d\tau$$

$$\le \exp\left(-\int_{s}^{t} b(\tau)\, d\tau \right) a(s) + \int_{s}^{t} c(\tau)\, d\tau \qquad (A5)$$

employing the mean-value theorem [39].

Because $\int_{t_0}^{\infty} b(t)\, dt = \infty$ and $b(t)$ is bounded, $\int_{s}^{\infty} b(t)\, dt = \infty$ and (A5) implies that $\limsup_{t \to \infty} a(t) \le \int_{s}^{\infty} c(\tau)\, d\tau$ for all $s \ge t_0 \ge 0$. Since $\int_{t_0}^{\infty} c(t)\, dt < \infty$, $\lim_{s \to \infty} \int_{s}^{\infty} c(t)\, dt = 0$ (see [29]) and hence we have $\lim_{t \to \infty} a(t) = 0$.

This completes the proof. ∎

Before proving Theorem 1, the following lemma is needed.

Lemma 6: Consider the tracking error model (5) with the control laws defined in (9) and (14). Let $\overline{x}_0$ be the new variable defined in (12). Then

1) $\lim_{t \to \infty} \overline{x}_0(t) = 0$;
2) There exists a constant $0 < T < \infty$ such that $|x_0(t)| \le 1$ and $|k_1 \overline{x}_0(t)| \le b$ for all $t \ge T_0$ and $\overline{x}_0(t)$ exponentially decays to zero when $t \ge T_0$;
3) Trajectories of the closed-loop system are all bounded before the time T_0.

Proof of Lemma 6:

1) It is trivial by (15) and (16).
2) From 1), it is clear that there is a constant $0 < T_0 < \infty$ such that $|\overline{x}_0(t)| \le 1 - \varepsilon(1 + \gamma)$ and $|k_1 \overline{x}_0(t)| \le b$ for all $t \ge T_0$. Then $|x_0(t)| \le |\overline{x}_0(t)| + \varepsilon(1 + \gamma) \le 1$ for all $t \ge T_0$. Note that $\dot{\overline{x}}_0 = -\alpha(x_1, x_2, t) k_1 \overline{x}_0$ for all $|k_1 \overline{x}_0| \le b$. Clearly, $\overline{x}_0(t)$ will exponentially decay to zero.
3) Now, let us prove the boundedness of (x_1, x_2). Let M be a positive number such that $0 \le v_r(t) \le M$, for all $t \ge 0$. Note that (11) gives

$$\dot{V}_1 \le 2|x_1| v_r \le 2(x_1^2 + x_2^2)^{1/2} M = 2(V_1)^{1/2} M. \qquad (A6)$$

We then have

$$V_1^{1/2}(t) \le V_1^{1/2}(0) + Mt < \infty, \qquad \forall\, t \in (0, T_0]. \qquad (A7)$$

Since $V_1(x_1, x_2)$ is positive-definite and radially unbounded, we conclude that trajectories $x_1(t)$ and $x_2(t)$ are bounded for all $0 \le t \le T_0$. This completes the proof. ∎

Now, we are ready to prove Theorem 1.

B. Proof of Theorem 1

Note that the coordinate transformation

$$(\overline{x}_0, x_1, x_2) = \left(x_0 + \frac{\varepsilon h x_1}{1 + V^{1/2}}, x_1, x_2 \right)$$

is invertible and $(\overline{x}_0, x_1, x_2) = (0, 0, 0)$ results in $(x_0, x_1, x_2) = (0, 0, 0)$. Thus, studying the stability of the error model (5a)–(5c), is equivalent to studying the stability of the cosystem consisting of (13) and (5b)–(5c). From Lemma 6, we conclude that the trajectories $\overline{x}_0(t)$, $x_1(t)$ and $x_2(t)$ are bounded and defined for all $0 \leq t \leq T_0$. In addition, equation (11) can be rewritten as

$$\dot{V}_1 = -2sat_a(k_0x_2)x_2 + 2v_rx_1\frac{\sin x_0}{x_0}$$
$$\cdot \left(x_0 + \frac{\varepsilon h x_1}{1 + V_1^{1/2}} - \frac{\varepsilon h x_1}{1 + V_1^{1/2}} \right)$$
$$\leq -2sat_a(k_0x_2)x_2 - v_r\frac{\varepsilon h x_1^2}{1 + V_1^{1/2}} + 2v_r|\overline{x}_0|\,|x_1|$$
$$\leq -2sat_a(k_0x_2)x_2 - v_r\frac{\varepsilon h x_1^2}{1 + V_1^{1/2}} + 2v_r|\overline{x}_0|V_1^{1/2} \quad \text{(A8)}$$

for all $t \geq T_0$ by 2) of Lemma 6 and the fact $(\sin x_0/x_0) \geq (1/2) \, \forall |x_0| \leq 1$. From Lemma 6, it is known that $\overline{x}_0(t)$ converges to zero exponentially when $t \geq T_0$. Thus

$$\int_0^\infty 2v_r|\overline{x}_0|\,dt < \infty. \quad \text{(A9)}$$

By Lemma 4, we conclude that
1)
$$V_1^{1/2}(t) \leq V_1^{1/2}(T_0) + \int_{T_0}^t v_r|\overline{x}_0(t)|\,dt \qquad \forall t \geq T_0$$

and
2)
$$\int_{T_0}^\infty \left(2sat_a(k_0x_2)x_2 + v_r\frac{\varepsilon h x_1^2}{1 + V_1^{1/2}} \right) dt$$
$$= \int_{T_0}^\infty 2sat_a(k_0x_2)x_2\,dt + \int_{T_0}^\infty v_r\frac{\varepsilon h x_1^2}{1 + V_1^{1/2}}\,dt < \infty.$$

The former tells us that the trajectories of the closed-loop system are also bounded after time T_0. Since $\dot{x}_2(t)$ is bounded, $x_2(t)$ is uniformly continuous. Using the result of Lemma 1 (Barbalat's Lemma) and 2), we have $\lim_{t\to\infty} x_2(t) = 0$ and hence there is a constant $0 < T_0 \leq T_1 < \infty$ such that $|k_0x_2(t)| \leq a$ for all $t \geq T_1$. In the following, let us divide our discussion into two cases.

1) $\int_{T_1}^\infty v_r(t)\,dt = \infty$.
   We have

$$\dot{V}_1 \leq -2k_0x_2^2 - v_r\frac{\varepsilon h x_1^2}{1 + V_1^{1/2}} + 2v_r|\overline{x}_0|V_1^{1/2}$$
$$\leq -v_r\left(\frac{2k_0x_2^2}{M} + \frac{\varepsilon h x_1^2}{1 + V_1^{1/2}} \right) + 2v_r|\overline{x}_0|V_1^{1/2}$$
$$\leq -\rho v_r V_1(x_1, x_2) + 2v_r|\overline{x}_0|V_1^{1/2}$$

for all $t \geq T_1$, where $\rho = \min\,((2k_0/M), (\varepsilon(1 - \gamma)/m)) > 0$ with $m = \sup_{t\geq0}(1 + V_1^{1/2}) < \infty$ and $v_r(t) \leq M, \forall t \geq 0$. Lemma 5 and (A9) give us $\lim_{t\to\infty} V_1(x_1, x_2) = 0$ and lead to $\lim_{t\to\infty} x_1(t) = 0$

and $\lim_{t\to\infty} x_2(t) = 0$. From the definition of $V_1(t)$ and Lemma 6, it follows that $\overline{x}_0(t)$, $x_1(t)$ and $x_2(t)$ will converge to zero. This implies that $\lim_{t\to\infty}|x(t) - x_r(t)| = 0$, $\lim_{t\to\infty}|y(t) - y_r(t)| = 0$, and $\lim_{t\to\infty}|\theta(t) - \theta_r(t)| = 0$ by the invertibility of coordinate transformation. So the TPSC is solved in this case. Note that the condition $\int_{T_1}^\infty v_r(t)\,dt = \infty$ is equivalent to $\int_0^\infty v_r(t)\,dt = \infty$ by the boundedness of v_r. The proof does not use any information regarding the constant μ. In particular, the TPSC is also solved under condition (C1) if μ is chosen as one.

2) $\int_{T_1}^\infty v_r(t)\,dt < \infty$
   In this case, it is well known that $\lim_{t\to\infty} v_r(t) = 0$ by Barbalat's lemma (Lemma 1). From the previous discussion, we have $\lim_{t\to\infty} x_2(t) = 0$ by Barbalat's lemma. We only have to prove that $\lim_{t\to\infty} x_1(t) = 0$ in view of Lemma 6.

Because of $sat_a(k_0x_2) = k_0x_2$ for $t \geq T_1$, system (5b)–(5c) with control law (9) can be written as

$$\dot{x}_1 = (w_r - u_0)x_2 + v_r\sin x_0 \quad \text{(A10a)}$$
$$\dot{x}_2 = -(w_r - u_0)x_1 - k_2x_2. \quad \text{(A10b)}$$

Using Lemma 2, we have

$$\lim_{t\to\infty} (w_r(t) - u_0(t))x_1(t) = 0. \quad \text{(A11)}$$

First, let us claim that there is a sequence $\{t_n\}$ of real numbers such that $\lim_{n\to\infty} t_n = \infty$ and $\lim_{n\to\infty} x_1(t_n) = 0$. Note that $sat_b(k_1\overline{x}_0) = k_1\overline{x}_0$ for all $t \geq T_1 \geq T_0$. If the claim is false, there are two constants $\varsigma > 0$ and $T' \geq T_1 > 0$ such that $|x_1(t)| \geq \varsigma, \forall t \geq T'$. Then, $\lim_{t\to\infty}(w_r(t) - u_0(t)) = 0$, i.e.,

$$\lim_{t\to\infty} \left| \frac{-\beta(x_0, x_1, x_2, t)}{\alpha(x_1, x_2, t)} - k_1\overline{x}_0 - w_r(t) \right| = 0 \quad \text{(A12)}$$

by (14) and (A11). Since $x_2 \to 0$ and $\overline{x}_0 \to 0$, (A12) can be reduced to

$$\lim_{t\to\infty} \left(w_r(t) + \frac{\varepsilon \dot{h}(t)x_1(t)}{1 + |x_1(t)|} \right) = 0 \quad \text{(A13)}$$

by Lemma 3. If condition (C2) holds, i.e., $\lim_{t\to\infty} w_r(t) = 0$, we will have

$$\lim_{t\to\infty} \left(\frac{\varepsilon \dot{h}(t)x_1(t)}{1 + |x_1(t)|} \right) = 0$$

by (A13). The fact that $|x_1(t)| \geq \varsigma, \forall t \geq T'$, and that $\mu = 1$ implies that $\lim_{t\to\infty}\dot{h}(t) = -\lim_{t\to\infty}\gamma\sin t = 0(\gamma > 0)$. Thus, we reach a contradiction. If condition (C3) holds [i.e., $\lim_{t\to\infty}\inf|w_r(t)| > 0$, and μ is chosen as one], and then

$$\lim_{t\to\infty} \inf \left| \frac{\varepsilon \dot{h}(t)x_1(t)}{1 + |x_1(t)|} \right| > 0$$

by (A13). However, $\lim_{n\to\infty}\dot{h}(n\pi) = \lim_{n\to\infty}\gamma\sin(n\pi) = 0$ by the choice of $\mu = 1$. We reach another contradiction. Note that condition (C1) does not hold in case 2). If conditions (C2)–(C3) do not hold, in particular, $\mu = 0$ and $h(t) = 1 + \gamma$ by the choice of μ, then this gives $\dot{h}(t) = 0$ and $\lim_{t\to\infty} w_r(t) = 0$, i.e., condition (C2) holds, by (A13).

We reach a contradiction. Thus, the claim is true. The claim implies that $\lim_{n\to\infty} V_1 x_1(t_n), x_2(t_n)) = 0$. We have $\lim_{t\to\infty} V_1(x_1(t), x_2(t)) \leq \lim_{n\to\infty} V_1(x_1(t_n), x_2(t_n)) = 0$ by inequalities (A8) and (A9). So, we can conclude that $\lim_{t\to\infty} \overline{x}_0(t) = 0$, $\lim_{t\to\infty} x_1(t) = 0$, and $\lim_{t\to\infty} x_2(t) = 0$. That is, $\lim_{t\to\infty} |x(t) - x_r(t)| = 0$, $\lim_{t\to\infty} |y(t) - y_r(t)| = 0$, and $\lim_{t\to\infty} |\theta(t) - \theta_r(t)| = 0$ again by the invertability of coordinate transformation. Therefore, the TPSC is also solved in this case and hence this completes the proof. ∎

REFERENCES

[1] S. Bentalba, A. E. Hajjaji, and A. Rachid, "Fuzzy control of a mobile robot: A new approach," in *Proc. IEEE Conf. Contr. Applicat.*, Hartford, CT, Oct. 1997, pp. 69–72.

[2] R. Biewald, "A neural network controller for the navigation and obstacle avoidance of a mobile robot," in *Neural Network for Robotic Control*, A. Zalzala and A. Morris, Eds. Singapore: Ellis Horwood, 1996, pp. 162–191.

[3] A. M. Bloch and N. H. McClamroch, "Control of mechanical systems with classical nonholonomic constraints," in *Proc. IEEE Conf. Decision Contr.*, Tampa, FL, 1989, pp. 201–205.

[4] A. M. Bloch, N. H. McClamroch, and M. Reyhanoglu, "Controllability and stabilizability of properties of a nonholonomic control systems," in *Proc. IEEE Conf. Decision Contr.*, Honolulu, HI, 1990, pp. 1312–1314.

[5] ——, "Control and stabilizability of nonholonomic Caplygin dynamic systems," in *Proc. IEEE Conf. Decision Contr.*, Brighton, U.K., 1991, pp. 1127–1132.

[6] A. M. Bloch, M. Reyhanoglu, and N. H. McClamroch, "Control and stabilizability of nonholonomic dynamic systems," *IEEE Trans. Automat. Contr.*, vol. 37, pp. 1746–1757, 1992.

[7] A. M. Bloch and S. Drakunov, "Stabilization of a nonholonomic system via sliding modes," in *Proc. 33rd IEEE Conf. Decision Contr.*, Lake Buena Vista, FL, 1994, pp. 2961–2963.

[8] ——, "Tracking in nonholonomic dynamic system via sliding modes," in *Proc. 34rd IEEE Conf. Decision Contr.*, New Orleans, LA, 1995, pp. 2103–2106.

[9] R. W. Brockett, "Asymptotic stability and feedback stabilization," in *Differential Geometric Control Theory*, R. W. Brockett, R. S. Millman, and H. H. Sussmann, Eds., 1983, pp. 181–191.

[10] C. de Wit Canudas, B. Siciliano, and G. Bastin, Eds., *Theory of Robot Control*. New York: Springer-Verlag, 1996.

[11] C. C. Chang and K. T. Song, "Environment prediction for a mobile robot in a dynamic environment," *IEEE Trans. Robot. Automat.*, vol. 13, pp. 862–872, 1997.

[12] E. D. Dickmanns, B. Mysliwetz, and T. Christians, "An integrated spatio-temporal approach to automatic visual guidance of autonomous vehicles," *IEEE Trans. Syst. Man Cybern.*, vol. 20, pp. 1273–1284, 1990.

[13] A. W. Divelbiss and J. T. Wen, "Trajectory tracking control of a car-trailer system," *IEEE Trans. Contr. Syst. Technology*, vol. 5, pp. 269–278, 1997.

[14] R. Fierro and F. L. Lewis, "Control of a nonholonomic mobile robot: backstepping kinematics into dynamics," in *Proc. 34th IEEE Conf. Decision Contr.*, New Orleans, LA, 1995, pp. 3805–3810.

[15] P. Fiorini and Z. Shiller, "Motion planning in dynamic environments using the relative velocity paradigm," in *Proc. IEEE Int. Conf. Robot. Automat.*, Atlanta, GA, 1993, pp. 560–565.

[16] ——, "Motion planning in dynamic environments using velocity obstacles," *Int. J. Robot. Res.*, vol. 17, no. 7, pp. 760–772, 1998.

[17] M. Fliess, J. Levine, P. Martin, and P. Rouchon, "Design of trajectory stabilizing feedback for driftless flat systems," in *Proc. 3rd Eur. Contr. Conf.*, Rome, Italy, 1997, pp. 1882–1887.

[18] J. Guldner and V. I. Utkin, "Stabilization of nonholonomic mobile robots using Lyapunov functions for navigation and slide model control," in *Proc. 33rd IEEE Conf. Decision Contr.*, Lake Buena Vista, FL, 1994, pp. 2967–2972.

[19] S. Ishikawa, "A method of indoor mobile robot navigation by fuzzy control," in *Proc. Int. Conf. Intell. Robot. Syst.*, Osaka, Japan, 1991, pp. 1013–1018.

[20] Z. P. Jiang and H. Nijmeijer, "Tracking control of mobile robots: A case study in backstepping," *Automatica*, vol. 33, pp. 1393–1399, 1997.

[21] ——, "A recursive technique for tracking control of nonholonomic systems in chained form," *IEEE Trans. Automat. Contr.*, vol. 44, pp. 265–279, 1999.

[22] Z. P. Jiang and J. B. Pomet, "Combining backstepping and time-varying techniques for a new set of adaptive controllers," in *Proc. IEEE Conf. Decision Contr.*, Lake Buena Vista, FL, 1994, pp. 2207–2212.

[23] Y. J. Kanayama, Y. Kimura, F. Miyazaki, and T. Noguchi, "A stable tracking control scheme for an autonomous mobile robot," in *Proc. IEEE Int. Conf. Robot. Automat.*, 1990, pp. 384–389.

[24] Y. J. Kanayama and B. I. Hartman, "Smooth local-path planning for autonomous vehicles," *Int. J. Robot. Res.*, vol. 16, no. 3, pp. 263–283, 1997.

[25] K. J. Kyriakopoulos and G. N. Saridis, "An integrated collision prediction and avoidance scheme for mobile robots in nonstationary environments," in *Proc. IEEE Int. Conf. Robot. Automat.*, Nice, France, 1992, pp. 194–199.

[26] J. F. G. de Lamadrid and N. L. Gini, "Path tracking through uncharted moving obstacles," *IEEE Trans. Syst., Man, Cybern.*, vol. 20, pp. 1408–1422, 1990.

[27] J. P. Laumond, P. E. Jacobs, M. Taix, and R. M. Murray, "A motion planner for nonholonomic mobile robots," *IEEE Trans. Robot. Automat.*, vol. 10, pp. 577–593, 1994.

[28] T. C. Lee, "Detectability, attractivity and invariance principle for nonlinear time-varying systems," in *Proc. 1998 R.O.C. Automat. Contr. Conf.*, Yunlin, Taiwan, R. O. C., Apr. 1998, pp. 401–406.

[29] T. C. Lee, C. H. Lee, and C. C. Teng, "Tracking control of mobile robots using the backstepping technique," in *Proc. 5th Int. Conf. Contr., Automat., Robot. Vision*, Singapore, Dec. 8–11, 1998, pp. 1715–1719.

[30] T. C. Lee, K. T. Song, C. H. Lee, and C. C. Teng, "Tracking control of mobile robots using saturation feedback controller," in *Proc. IEEE Int. Conf. Robot. Automat.*, Detroit, MI, May 1999, pp. 2639–2644.

[31] Y. Ma, J. Kosecka, and S. Sastry, "Vision guided navigation for a nonholonomic mobile robot," in *Proc. IEEE 36th Conf. Decision Contr.*, San Diego, CA, 1997, pp. 3069–3074.

[32] R. T. M'Closkey and R. M. Murray, "Exponential stabilization of nonlinear driftless control systems via time-varying homogeneous feedback," in *Proc. IEEE Conf. Decision Contr*, Lake Buena Vista, 1994, pp. 1317–1322.

[33] ——, "Exponential stabilization of driftless control systems using homogeneous feedback," *IEEE Trans. Automat. Contr.*, vol. 42, no. 5, pp. 614–628, 1997.

[34] R. M. Murray, G. Walsh, and S. S. Sastry, "Stabilization and tracking for nonholonomiccontrol systems using time-varying state feedback," in *IFAC Nonlinear Control Systems Design*, M. Fliess, Ed. CITY OF PUBLISHER???: Bordeaux, 1992, pp. 109–114.

[35] R. M. Murray and S. S. Sastry, "Nonholonomic motion planning: Steering using sinusoids," *IEEE Trans. Automat. Contr.*, vol. 38, pp. 700–716, 1993.

[36] W. Oelen and J. van Amerongen, "Robust tracking control of two-degree-freedom mobile robots," *Contr.l Eng. Practice*, vol. 2, pp. 333–340, 1994.

[37] D. A. Pomerleau, *Neural Network Perception for Mobile Robot Guidance*. Boston, MA: Kluwer, 1993.

[38] J. B. Pomet, "Explicit design of time-varying stabilizing control laws for a class of controllable systems without drift," *Syst. Contr. Lett.*, vol. 18, pp. 467–473, 1992.

[39] W. Rudin, *Real and Complex Analysis*. New York: McGraw-Hill, 1987.

[40] C. Samson and K. Ait-Abderrahim, "Feedback control of a nonholonomic wheeled cart in cartesian space," in *Proc. IEEE Int. Conf. Robot. Automat.*, Sacramento, CA, 1991, pp. 1136–1141.

[41] C. L. Shih, T. Lee, and W. A. Gruver, "A unified approach for robot motion planning with moving polyhedral obstacles," *IEEE Trans. Syst., Man, Cybern.*, vol. 20, no. 4, pp. 903–915, 1990.

[42] J. J. Slotine and W. Li, *Applied Nonlinear Control*. Englewood Cliffs, NJ: Prentice-Hall, 1991.

[43] K. T. Song and W. H. Tang, "Environment perception for a mobile robot using double ultrasonic sensors and a CCD camera," *IEEE Trans. Ind. Electron.*, vol. 43, no. 3, pp. 372–379, 1996.

[44] K. T. Song and C.E. Li, "Tracking control of a fee ranging automatic guided vehicle," *Contr. Eng. Practice*, vol. 1, no. 1, pp. 163–169, 1993.

[45] K. T. Song and L.H. Sheen, "Heuristic fuzzy-neuro network and its application to reactive navigation of a mobile robot," *Fuzzy Sets Systems*, vol. 110, no. 3, pp. 331–340, 2000.

[46] C. J. Taylor and D. J. Kriegman, "Vision-based motion planning and exploration algorithms for mobile robots," *IEEE Trans. Robot. Automat.*, vol. 14, pp. 417–426, 1998.

Ti-Chung Lee was born in Taiwan, R.O.C., in 1966. He received the M.S. degree in mathematics from the National Tsing Hua University, Hsinchu, Taiwan, R.O.C., in 1990 and the Ph.D. degree in electrical engineering from the National Tsing Hua University, in 1995.
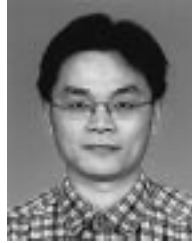
He is currently an Assistant Professor of the Department of Electrical Engineering, Ming Hsin Institute of Technology. His main research interests are nonlinear control systems, nonholonomic systems and robot control.

Ching-Hung Lee was born in Taiwan, R.O.C., in 1969. He received the B.S. and M.S. degree in control engineering from the National Chiao Tung University, Hsinchu, Taiwan, R.O.C., in 1992 and 1994, respectively, and the Ph.D. degree in electrical and control engineering from the National Chiao Tung University in 2000.

He is currently an Assistant Professor of the Department of Electronic Engineering at Lunghwa Institute of Technology. His main research interests are fuzzy neural systems, fuzzy logic control, neural network, signal processing, nonlinear control systems, and robot control.

Kai-Tai Song (A'91) was born in Taipei, Taiwan, R.O.C., in 1957. He received the B.S. degree in power mechanical engineering from National Tsing Hua University in 1979 and the Ph.D. degree in mechanical engineering from the Katholieke Universiteit Leuven, Belgium, in 1989.

He was with the Chung Shan Institute of Science and Technology from 1981 to 1984. Since 1989 he has been on the faculty and is currently a Professor in the Department of Electrical and Control Engineering, National Chiao Tung University, Taiwan. His areas of research interest include mobile robots, image processing, visual tracking, sensing and perception, embedded systems, intelligent system control integration, and mechatronics.

Ching-Cheng Teng was born in Taiwan, R.O.C., in 1938. He received the B.S. degree in electrical engineering from the National Cheng Kung University, Taiwan, in 1961.

From 1991 to 1998, he was the Chairman of the Department of Electrical and Control Engineering, National Chiao Tung University. He is currently a Professor of the Department of Electrical and Control Engineering at National Chiao Tung University. His research interests include optimal control, signal processing, and fuzzy neural systems.